Petroleum and Coal

Article **Open Access**

Studying of the Processing of Fluid Catalytic Cracking Slurry Oil in the H-Oil Ebullated Bed Vacuum Residue Hydrocracking and Its Effect on the H-Oil Vacuum Gas Oil Quality and Fluid Catalytic Cracking Performance

Dicho Stratiev[1], Ivelina Shishkova[1], Rosen Dinkov[1], Dobromir Yordanov[2]

[1] *LUKOIL Neftohim Burgas, Burgas 8104, Bulgaria*
[2] *University "Prof. Dr. Assen Zlatarov", Burgas 8000, Bulgaria*

Received February 25, 2020; Accepted April 22, 2020

Abstract

Investigation on the properties of fluid catalytic cracking (FCC) slurry oil (SLO) at different conversion levels and the impact of FCC SLO processing on H-Oil vacuum residue hydrocracking performance and on the subsequent performance of the FCC unit was carried out in this paper. Analysis of FCC SLO samples taken at different FCC conversion levels did not show any effect of conversion on the FCC SLO properties in the FCC conversion range 72.47-82.4%. The addition of FCC SLO to the H-Oil feed reduced sediment level in the atmospheric tower bottom (ATB) product, which is in line with other research reports. The distribution of FCC SLO among the H-Oil products was following: 15% in vacuum tower bottom (VTB) product; 60% in vacuum gas oil (VGO) product), and 25% in diesel product. The increase of the amount FCC SLO in H-Oil feed decreases the FCC conversion, and the yields of the higher value products: C_3 cut, C_4 cut, and gasoline, and increases the yields of the lower value products: heavy cycle oil (HCO) , and SLO. An optimized balance between H-Oil VR hydrocracker and VGO FCC unit performance related to the optimum amount of FCC SLO processed in the H-Oil could improve the performance of the whole refinery.

Keywords: *Fluid catalytic cracking; Ebullated bed vacuum residue hydrocracking slurry oil; Conversion; Sediments.*

1. Introduction

The fluid catalytic cracking (FCC) slurry oil (some call this product as FCC decant oil, clarified oil, FCC bottoms or heavy cycle oil) is the heaviest product obtained during catalytic cracking of heavy atmospheric gas oil, vacuum gas oil, and sometimes atmospheric resid [1]. Due to its overwhelmingly aromatic nature this complex mixture cannot be used as automotive fuels [2-3]. Generally, it is mixed into heavy fuel oil as a viscosity cutter [4]. The FCC slurry oil (SLO) is a low molecular weight product with high aromaticity and short side chain [5]. The reported values for the density at 15°C of the FCC SLO, which is an indicator for the aromaticity [6-7], vary between 0.9594 [3] to 1.126 g/cm^3 [1]. The reported values for the aromatics content of the FCC SLO vary between 54.1 [3] to 99.2% [2]. It was found that the FCC slurry hydrogen content strongly correlates with the aromatics content determined by ASTM D-2549 (Fig.1 a) and it can vary between 6.9 and 11.7% [2]. The FCC SLO molecular weight was found to correlate with the number of carbon atoms in alkyl side chains (Fig. 1 c) [7] and with the aromatics content (Fig.1 d) [2]. This suggests that with the evolution of the catalytic cracking of the heavy oil (increase of conversion) the FCC SLO becomes a lower molecular weight heavy oil fraction due to the scission of the side alkyl chains attached to the aromatic cores, which become shorter, and due to the cracking of the alkanes, which disappear from the FCC SLO contents. One may conclude that density, or hydrogen content of the FCC SLO are sufficient indicators for its aromatics content and the degree of aromatic condensation and they are interrelated with each other as deduced from Figures 1 and 2 [7]. The higher aromaticity of the FCC SLO [8] makes this material desirable for the addition to the vacuum residue hydrocracking because it has a positive effect (decreasing) on the sediment formation in the hydrocracker [9-13].

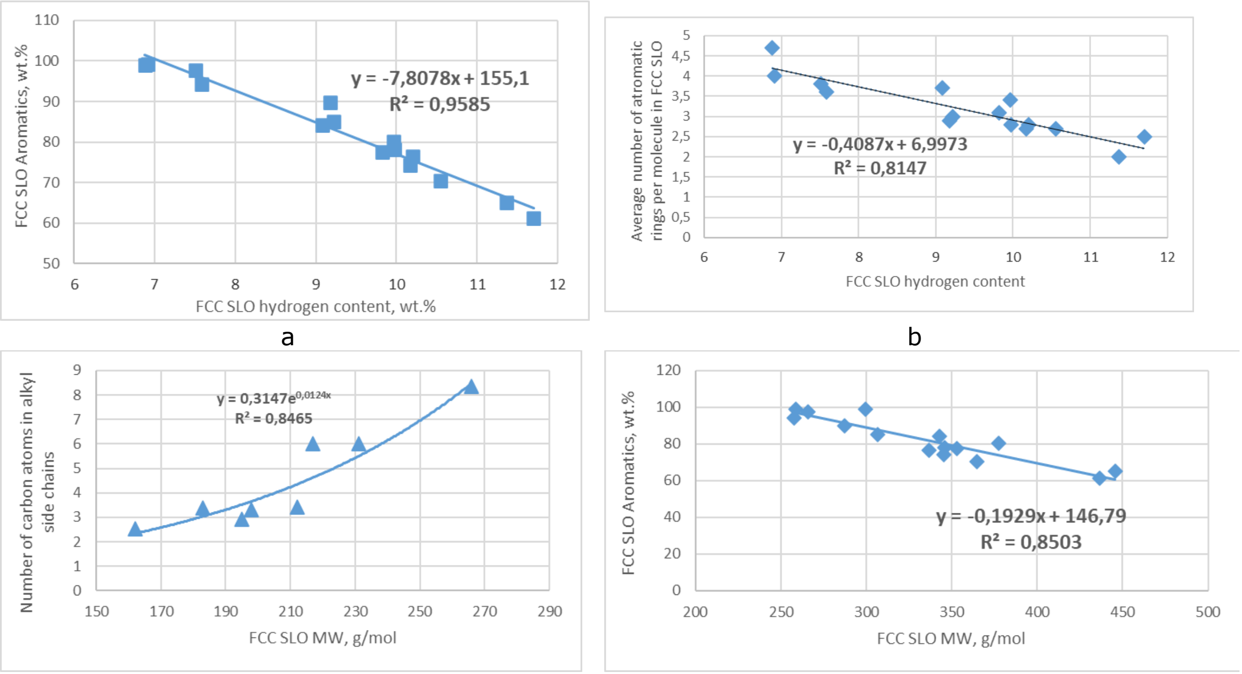

a b

c d

Figure 1 Relations of FCC SLO hydrogen content to aromatics content and the average number of aromatic rings per molecule, and relations of FCC SLO molecular weight to the FCC SLO aromatics content and the number of carbon atoms in alkyl side chains (Data extracted from refs 2 and 7)

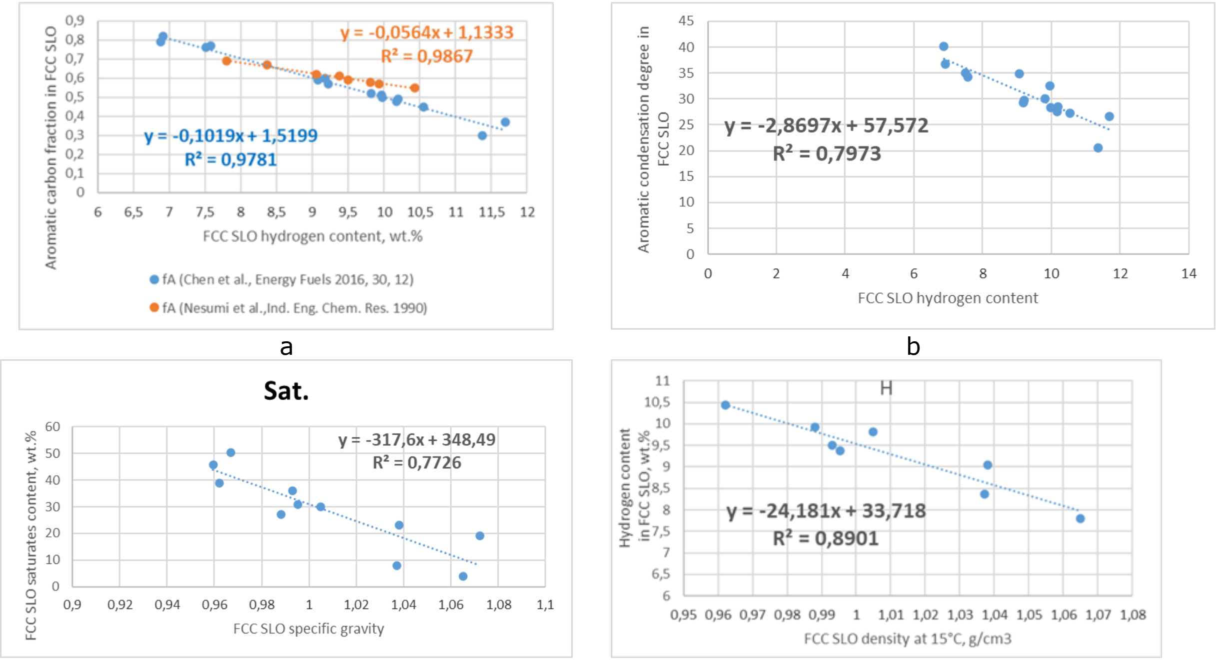

a b

c d

Figure 2 Figure 1 Relations of FCC SLO hydrogen content to aromatics carbon fraction (a), to aromatic condensation degree (b), to density (d), and a relation of FCC SLO density to saturate content (Data extracted from refs 2 and 7)

However, the FCC SLO, despite its high aromatics content, is not always suitable for hydroprocessing, especially when it is blended with materials like high high saturate content virgin gas oils in a great amounts [14]. In such a case a plugging of the catalyst bed in a fixed-bed hydrotreater was reported [14]. Another example showing that the addition of the FCC SLO can destroy the colloidal stability and increase the particle size of aggregated asphaltenes is the addition of FCC SLO to Tahe atmospheric residue as reported in [15]. It was found in that study that the decline of the colloidal stability of Tahe atmospheric residue was attributed to the component polarity difference between oil fractions and the atmospheric residue. The polarity of aromatics and resins of FCC slurry oil was lower than that of Tahe atmospheric residue, which was found to be the reason for the deteriorated colloidal stability. The addition of FCC decant oil (SLO) to a heavy crude oil in amount 10% was reported by Tirado and Ancheyta to increase the sediment level during hydroprocessing, while the lower molecular weight FCC gas oils LCO and HCO decreased the sediment content [16]. They concluded that both the high concentration of aromatic compounds and their structure are the factors responsible for the decrease in sediment formation. The FCC decant oil used by Tirado and Ancheyta was heavier than that reported by other researchers having higher amount of complex molecules like poly-aromatics, which may explain the increased tendency of the FCC decant oil to form sediments [16].

One of the option to convert the lower value FCC SLO to higher value products is to recycle and process it with a fresh FCC feed [17]. Unfortunately due to the large amount of poly-nuclear aromatics (PNA) in the FCC SLO it is difficult to convert, and the FCC SLO PNA tend to undergo condensation coking reactions during the catalytic conversion [17-20]. It was found that during catalytic cracking of PNAs very little cracking of the 2-ring PNA over the FCC catalyst occurred, while in contrast the 3-ring PNA was highly reactive, and was rapidly converted into monocyclic aromatic hydrocarbons, 2-ring PNAs and coke. As a whole the higher propensity to form coke of the FCC SLO limits its processing in the commercial FCC unit because the regenerator temperatures may go beyond the metallurgical limit of the regenerator vessel. A selective hydrogenation of the FCC SLO could increase its conversion from 39.7 to 63.5 wt.% [21]. It was shown that tetralin-type naphthenoaromatics were the desired hydrogenation products, which provide a low selectivity of coke and heavy oil [21]. The selective hydrogenation of FCC SLO was also shown to increase its hydrogen-donating ability and thereby becoming an optimal hydrogen donor solvent for asphaltenes conversion during hydroconversion experiments [22]. The naphthenebenzenes obtained by hydrogenation of the PNA was found to have the maximal HAD and they were the component for hydrogen donating performance of Hy-HCO for asphaltenes hydroconversion [22].

There are applications for the FCC SLO which includes the use of FCC SLO as a blendstock for production of road asphalts [23-25]. Others involve hydrotreatment of FCC SLO [26-27] and subsequent carbonization to produce high needle coke [28]. The FCC SLO has been also studied as a feedstock for coke production [29-30], and for production of special products [31-34].

Marques et al. concluded that at HCO (SLO) contents lower than 15 vol %, in the vacuum residue hydrocracking feed, the HCO does not impact the 540°C+ conversion level or the hydrotreating performances of the residue-upgrading process [9]. Their work illustrated that the aromatic species of the HCO played an important role in the stabilization mechanisms but that the HCO does not participate in the hydroconversion reactions [9].

The aim of current work is to study what kind of transformations occur during processing FCC SLO in the H-Oil ebullated bed vacuum residue hydrocracking when the FCC SLO content in the H-Oil feed varies between 4 and 12%. How the processing of FCC SLO impacts the quality of H-Oil gas oils products (HAGO, LVGO, HVGO) and what is the effect of this on FCC conversion.

2. Experimental

All hydrocracking experiments were carried out at the LNB EBVR H-Oil hydrocracker. A simplified process diagram of the LNB EBR H-Oil hydrocracker is presented in [12]. Details about the LUKOIL Neftohim Burgas H-Oil residue hydrocracker are given in [12].

The vacuum residue 540°C+ conversion was estimated by the equation:

$$\text{Conversion}\ \ (\%) = \frac{EBRHCFeed_{540^\circ C+} - EBRHC\,\mathrm{Pr}oduct_{540^\circ C+}}{EBRHCFeed_{540^\circ C+}} \times 100$$

eq. (1)

where: $EBRHCFeed_{540^\circ C+}$ = mass flow rate of the EBVRHC feed fraction boiling above 540°C, determined by high temperature simulated distillation, method ASTM D 7169 of the feed and multiplied by the mass flow rate of the feed; $EBRHCProduct_{540^\circ C+}$ = mass flow rate of the EBVRHC product fraction boiling above 540°C, determined by high temperature simulated distillation, method ASTM D 7169 of the liquid product multiplied by the flow rate of the liquid product.

The operating conditions (reaction temperature, and reaction time) in the LNB EBVR H-Oil hydrocracker were varied in such a way to obtained a conversion that varied in the range 55-78%.

All cracking experiments have been performed at the LNB FCCU. Details about the LNB FCCU are presented in [35]. The FCC conversion was defined as 100-LCO-HCO-Slurry, %. The FCC LCO is a product with cut points of 210 and 300°C; FCC HCO is a product with cut points of 300 and 360°C; the FCC slurry is a product with cut point 360°C+. A correction of conversion to gasoline T90%=175°C was employed to account for the variation in the fractionation between gasoline and LCO FCC products.

3. Results and discussion

3.1. H-Oil operation severity impact on yields and quality of FCC gas oils

In our previous studies [36-37] we have shown that the H-Oil weight average bed temperature (WABT) has a direct impact on the conversion in the FCCU. The increase of H-Oil WABT leads to a decrease of FCCU conversion [37]. In Figure 3 a relation of H-Oil WABT to the yields of FCC gas oils is presented.

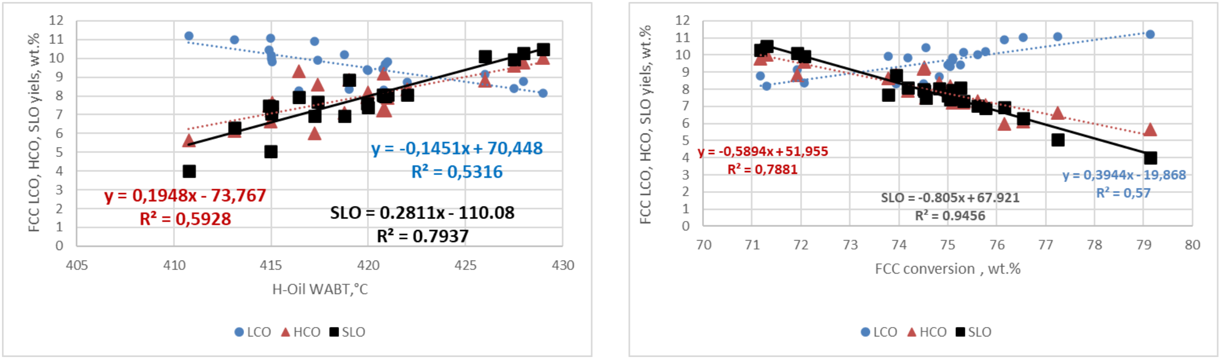

a b

Figure 3. Relation of H-Oil WABT to the yields of FCC gas oils (a), and relation of FCC feed conversion to the yields of FCC gas oils (b)

In Figure 3 b a relation of FCC feed conversion to the yields of FCC gas oils is depicted. This data clearly shows that the increase of H-Oil WABT decreases LCO yield and increases the yields of HCO, and SLO. The data in Figure 3 b indicate that the increase of conversion improves the yield of LCO. Our earlier study showed that the cracking of higher reactivity feeds leads to production of higher amount of LCO. Figure 4 indicates data for catalytic cracking, performed in an ACE laboratory FCC unit, of two feeds, which have different reactivity, as discussed in our recent study [38], and shown in Figure 4 a. The data in Figure 4 b exhibited that from the more reactive feed, which gives a higher conversion at the same reaction severity (the same CTO in that case), a higher yield LCO is obtained at the expense of the higher yield of SLO. Therefore, one may conclude that the increase of H-Oil WABT, not only decreases FCC conversion in the LNB FCC unit, but also decreases the yield of LCO at the expense of increasing the yields of HCO and SLO.

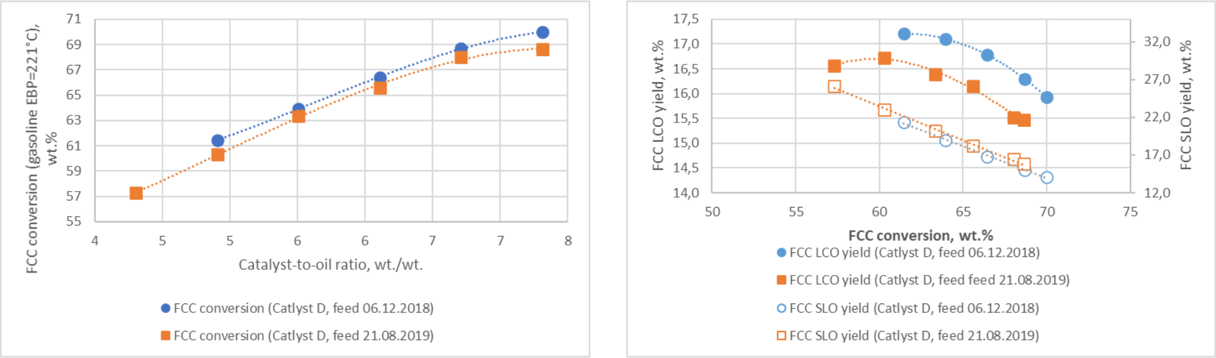

a

b

Figure 4. Dependence of FCC conversion on catalyst-to-oil ratio for two different feeds (a); FCC LCO yield as a function of the conversion for two different feeds

Table 1 presents data for the distillation characteristics, density, and viscosity of the LNB FCC gas oils (LCO, HCO, and SLO). Table 1 also includes data for FCC SLO molecular weight, estimated by Goosens' correlation [39], and hydrogen and aromatic carbon content, estimated by Conoco Philips method [40]. Table 1 also includes data for hydrogen content, measured by ASTM D 5291 [41], and for the heat of combustion for one SLO sample.

The relations of the distillation characteristics to density, and viscosity of the studied FCC gas oils have been examined by correlation matrix for these three FCC gas oils. These correlation matrices are presented in Table 2.

Table 2. Correlation matrices of properties of FCC gas oils under study

	LCO d15	*T5*	*T10*	*T50*	*T90*	*T95*	*VIS at 40*
FCC LCO d15	1						
T5	**0.91**	1.00					
T10	0.42	0.94	1.00				
T50	**0.84**	0.78	0.59	1.00			
T90	0.58	0.46	-0.04	0.72	1.00		
T95	0.62	0.44	0.57	0.87	1.00	1.00	
VIS at 40	**0.82**	0.58	0.62	**0.90**	**0.92**	**0.90**	1.00
	HCO d15	*T5*	*T10*	*T50*	*T90*	*T95*	*VIS at 40*
FCC HCO d15	1						
T5	-0.11	1.00					
T10	0.69	0.90	1.00				
T50	0.69	0.76	0.94	1.00			
T90	0.51	0.36	0.48	0.73	1.00		
T95	**0.85**	0.24	0.52	0.78	**0.99**	1.00	
VIS at 40	0.64	0.66	0.84	**0.96**	0.91	0.85	1.00
	SLO d15	*T5*	*T10*	*T50*	*T90*	*T95*	*VIS at 80*
FCC SLO d15	1.00						
T5	0.15	1.00					
T10	0.34	**0.87**	1.00				
T50	0.56	0.09	0.41	1.00			
T90	0.64	-0.05	-0.18	0.08	1.00		
T95	**0.77**	-0.17	-0.17	0.26	**0.93**	1.00	
VIS at 80	**0.99**	0.36	0.34	0.71	**0.76**	0.66	1.00

Table 1. Properties of FCC gas oils (LCO, HCO, SLO) sampled at different conversion levels from the LNB FCCU

Date	29.6.2012	2.7.2012	4.7.2012	23.1.2015	24.1.2015	26.1.2015	28.9.2015	13.11.2017	12.12.2018	22.1.2020	26.6.2017
FCC LCO d15, g/cm^3	0.9254	0.935	0.9188	0.9568	0.9484	0.9401	0.9556	0.9269	0.9386	0.9225	0.9283
T5%, °C	181	181	175	195	188	193				178	
T10%, °C	198	199	194	206	205	206	223.3	225.8	227.2	192	227
T50%, °C	242	251	231	253	251	249	254.4	243.7	251.5	227	246
T90%, °C	286	306	273	298	290	283	284.4	271.9	284.7	269	276
T95%, °C	298	320	283	309	301	295				279	
Kin. Vis. at 40°C, mm^2/s	1.9	2.2	1.8	2.22	2.1	1.98					
FCC HCO d15 g/cm^3	0.991	1.0025	0.9902	1.0236	1.01	0.9974			1.0054	1.0052	0.9924
T5%, °C	271	278	260	266	253	260				257	
T10%, °C	284	297	271	282	275	274			309.8	267	283
T50%, °C	325	342	315	332	325	318			344.3	316	328
T90%, °C	365	382	359	381	375	367			374.1	370	370
T95%, °C	378	394	373	396	391	382				383	
Kin. Vis. at 40°C, mm^2/s	8.6	12.4	7.6	11.61	8.9	8.0					
FCC SLO d15 g/cm^3	1.0564	1.0662	1.0615	1.0943	1.0779	1.0621	1.101	1.082	1.1149	1.0939	1.0970
T5%, °C	313	319	305	314	309	300	311	303	307	319	
T10%, °C	329	337	324	331	326	317	325	326	332	340	
T50%, °C	392	401	391	400	397	389	393	403	407	393	
T90%, °C	471	476	471	491	493	484	525	488	490	483	
T95%, °C	493	498	494	525	531	520	594	525	563	511	
Boiling below 360°C, wt.%	26	22	28	24	26	32	30	22	20	20	
Kin. Vis. at 80°C, mm^2/s	16.2	21.3	17.4	33.76	24.21	18.47					
Molecular weight, g/mol	258	265	255	257	258	253	248	263	259	250	
Hydrogen content, wt.%	8.4	8.2	8.3	7.4	7.9	8.2	7.2	7.8	6.9	7.4	8.0
Aromatic carbon content, wt.%	65	67	67	75	71	67	78	71	81	76	
Calorific data, MJ/kg											38.6
FCC TRX, °C	528	529	530	540	540	540	539	539	537	538	536
FCC Conv., wt.%	79.3	80.7	80.6	82.4	81.4	80.2	84.4	75.1	73.9	75.1	72.7

It is evident from the data in Table 2 that the density of LCO most strongly correlates with the $T_{5\%}$ of the distillation characteristics. This suggests that that the density of the LCO depends mainly on the fractionation between the cracked gasoline and the LCO from the LNB FCCU. Viscosity of the LCO most strongly correlates with $T_{90\%}$ of the distillation characteristics. Therefore, the viscosity of the FCC LCO is governed by the heavy part of this material. The data in Table 2 indicates that the FCC HCO density is governed by the heavier part of this FCC gas oil (R=0.85 for FCC HCO d_{15} with $T_{95\%}$ =0.85). The viscosity of FCC HCO most strongly correlates with $T_{50\%}$ (R=0.96). The data in Table 2 shows that the FCC SLO density most strongly correlates with viscosity (R=0.99) and a weaker correlation of the SLO d_{15} with $T_{95\%}$ (R=0.77) is registered. The data for the FCC SLO molecular weight presented in Table 1 shows that it varies in a narrow range, between 250 and 263 g/mol. It is much lower than the molecular weight of the LNB FCC VGO feed, which has 100 g/mol (MW=363 g/mol) higher molecular weight than the FCC SLO. This indicates that the catalytic cracking of the VGO breaks the side alkyl chains attached to the aromatic cores. This results in a lower molecular weight VGO boiling range product (that is FCC SLO) with much higher aromaticity, density, and viscosity. The data in Table 1 also indicate that the FCC SLO hydrogen content of the studied samples varied between 6.9 and 8.4. These values were obtained by the use of the Conoco Phillips correlation [40] and they well fit to the measured hydrogen content by the ASTM D 5291 of the FCC SLO sample from 26.6.2017. Therefore, we may consider these values as correct. If we use the correlation established from the NMR data for FCC SLO [2] and shown in Figure 1a we can find the LNB FCC SLO has a content of aromatic compounds according to ASTM D-2549 [42] of about 93%. The hydrogen content of about 8% corresponds to aromatic carbon fraction of about 0.7 as illustrated in Figure 2a. An average number of aromatic rings per molecule of about 3.7 is obtained for hydrogen content in the FCC SLO of about 8%, as shown from the data in Figure 1 b. For the molecular weight of the FCC SLO of about 257 the aromatic content according to the data in Figure 1 d corresponds to about 97%. In other words, the aromatics content in the FCC SLO produced at the LNB FCCU is higher than 90% and lies in the range between 92 and 97%. The data in Table 1 does not show any relation of the quality of the FCC SLO to the FCC reaction temperature in the studied range between 530 and 540°C. Neither a relation exists between the SLO and the FCC conversion in the studied range between 73.9 and 82.4%.

3.2. Effect of processing of FCC SLO in H-Oil on sedimentation, product yield structure and quality of the H-Oil gas oils (HAGO, LVGO, HVGO)

Marques et al. showed that the stability of the hydrocracked residual oils is being ruled by the maltene aromaticity, more specifically by the tetra- and penta-aromatics in the 350-540°C cut [9]. In their study the addition of the FCC SLO to the VR hydrocracking feed did not alter the nature of the hydrocracked asphaltenes but the composition of the product 350-540°C (VGO) cut varied significantly, leading to strongly varying sediment levels in the effluents [9].

Figure 3 demonstrates how the addition of about 8% of the total feed for the LNB H-Oil VR. The data in Figure 3 indicates that after addition of about 8% to the H-Oil feed the sediment content in the ATB product dropped from 0.4 down to 0.15%. at the same time the H-Oil WABT was increased from 423 up to 427°C. The decreased sediment content in the H-Oil ATB product, a result from insertion of 8% FCC SLO in the H-Oil feed is in line with the reports by other researchers [9-11].

Žajdlík, and Báhidský [43] reported that during processing of FCC SLO in the ebullated bed vacuum residue hydrocracking (LC-Fining) 80% of the FCC SLO ended up in the LC-Finer VGO product, and 20% remained in the VTB product. In order to understand the transformations which occur with FCC SLO during its processing in the LNB H-Oil hydrocracker a dedicated commercial test with and without processing of FCC SLO was performed. The test was performed at throughput of 245 t/h and WABT of 423°C for the case without FCC SLO processing and WABT of 425.5°C for the test with processing of 20 t/h FCC SLO.

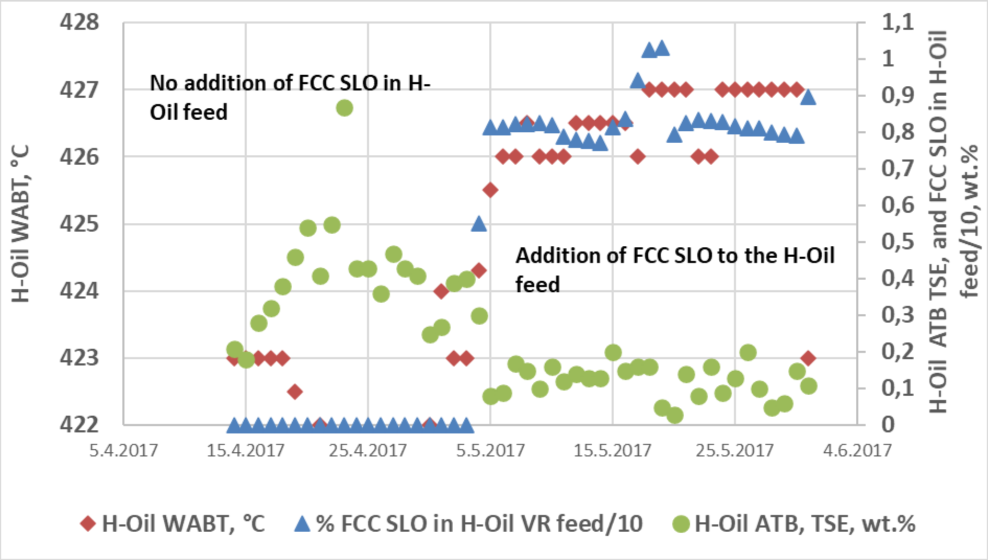

Figure 3 Effect of the addition of FCC SLO to the ATB sediment content (TSE) and H-Oil WABT before and after addition of FCC SLO in the H-Oil feed

Table 3 summarizes the results from this test. In order to compare the yields for both cases at the same WABT of 425.5°C the conversion at 423°C was transformed in conversion at 425.5°C using the data for the activation energy of Ea = 220.8 kJ/mole, and pre-exponential factor of $k_0=2.219*10^{16}$, determined in our recent study [44]. The yields from 100% VRO at WABT of 425.5°C were obtained by the use of the product selectivities estimated from the data for the case of WABT = 423°C and the estimated conversion at 425.5°C, as described earlier. The final result shows that the distribution of the FCC SLO among the H-Oil products is 24% going to diesel; 61% going to VGO; and 15% going to VTB. By employing eq.1 to estimate density of petroleum products blends:

$$Blend\ density = \frac{100}{\frac{Product1\%}{density1}+Product2\%/density2} \qquad \text{eq.(2)}$$

where: Blend density = density of the diesel, and VGO of these products obtained from hydrocracking of the feed VRO (92%) blended with FCC SLO (8%), g/cm^3 at 15°C; Product 1 % - FCC SLO content in the H-Oil diesel, and H-Oil VGO 5.8% and 15.5% respectively;

The data for densities 1 and 2 for eq.1 are given in Table 3 (the last two rows).

Using eq. 2 and the densities mentioned above the density of the material coming from the FCC SLO in the H-Oil diesel was found to be 0.943 g/cm^3. Comparing this value with the value for the density of the FCC HCO (Table 1) that is about 1.00 g/cm^3 some extent of hydrogenation of this material may be suggested. The density of the material coming from the FCC SLO in the H-Oil VGO was found to be 1.023 g/cm^3. Comparing this value with the value for the density of the FCC SLO (Table 1) that is about 1.09 g/cm^3 some extent of hydrogenation of this material may be suggested again. Our data are in line with those reported by Marques *et al.* [9] showing no hydroconversion of the FCC SLO (no increase in the yields of gas and naphtha, and the increase of the diesel yield is equivalent to the content of the fraction boiling below 360°C in the FCC SLO (about 24% see Table 1)). However, the reduction of the densities of the material from the FCC SLO in the H-Oil diesel and VGO of about 60-70 kg/m^3 suggests that some hydrogenation of the FCC SLO takes place at the conditions of the ebullated bed VR HC studied in this work. The increase of the content of FCC SLO in the H-Oil feed has an effect of proportional increasing of density of the three H-Oil gas oil products as illustrated in Figure 4. More data about the properties of H-Oil gas oils (HAGO, LVGO, HVGO) obtained during hydrocracking VRO feeds which contain different amount of FCC SLO are presented in Table 4.

Table 3. Results from the commercial test at the LNB H-Oil VR HC unit with and without processing FCC SLO

Characteristics	without FCC SLO	with FCC SLO	1	2	3	4	5	5
Throughput, t/h	245	245	H-Oil yields from 100% VRO at 75.1% conversion, %	Products in t/h from 225 t/h VRO	Products in t/h from 225 t/h VRO and 20 t/h FCC SLO	Δ (column 3-column 4)	Distribution of FCC SLO between H-Oil products,%	Density of the product coming from FCC SLO,g/cm^3
FCC SLO, t/h	0	20						
VRO, t/h	245	225						
WABT, °C	423	425.5						
Gas, wt.%	7.21	6.9	7.5	16.9	16.9	0.0		
Naphtha, wt.%	8.02	7.7	8.3	18.7	18.9	0.1		
Diesel, wt.%	33.16	33.6	34.4	77.5	82.3	4.8	23.6	0.943
VGO, wt.%	28.01	31.6	29.1	65.5	77.4	12.0	60.4	1.023
VTB, wt.%	22.48	19.3	19.7	44.3	47.3	3.0	15.4	
H_2S, wt.%	4.16	4.0						
Total, wt.%	103.0	103.1						
ATB, TSE, %	0.4	0.08				19.9	99.4	
H-Oil feed 540°C- content, wt.%	17.0	24.6						
H-Oil VTB 540°C- content, wt.%	16.5	17.2						
Net conversion,%	72.3	73.2						
Gas selectivity,%	10.0	9.4						
Naphtha selectivity, %	11.1	10.5						
Diesel selectivity,%	45.8	45.8						
VGO selectivity,%	38.7	43.0						
Expected conversion at WABT of 425.5°C,%	75.1							
Diesel density at 15°C, g/cm^3	0.8507	0.8556						
VGO density at 15°C, g/cm^3	0.9300	0.9430						

Product 2 %- H-Oil diesel, and H-Oil VGO content obtained from hydrocracking of 100% VRO; Density 1 = density of FCC SLO in the H-Oil diesel and of the H-Oil VGO (not known, which are searched), g/cm^3 at 15°C; Density 2 = H-Oil diesel, and H-Oil VGO obtained from hydrocracking of 100% VRO, g/cm^3 at 15°C.

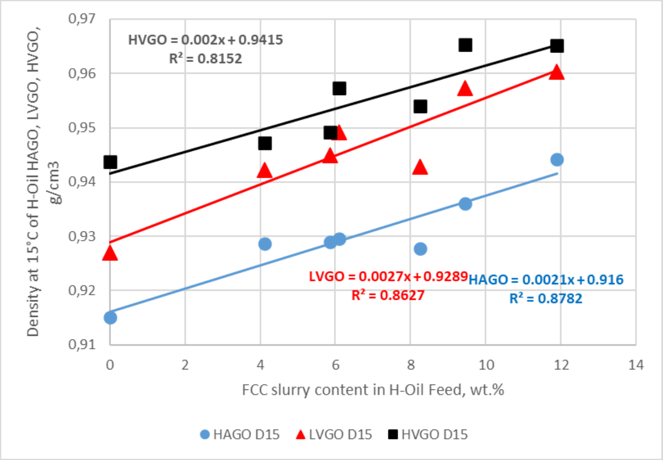

Figure 4 Relation of the content of FCC SLO in the LNB H-Oil VR feed to the density of the H-Oil gas oils (HAGO, LVGO, HVGO)

One may conclude that the FCC SLO increases the yield of H-Oil diesel since it contains about one fourth of diesel material, and increases the yield of H-Oil VGO since the FCC SLO is in fact VGO. Some small amount of it ends up in the VTB, which depends on the fractionation efficiency of the H-Oil vacuum tower. Figure 5 presents graphs of selectivity curves for the vacuum residue hydrocracking products obtained in a laboratory hydrocracking unit, as described in [45], and in the commercial LNB H-Oil VR hydrocracker. The VRHC product yields distribution, as shown in Figure 5 a [45] can be described as that explained in the work of Wallenstein and Alkemade [46] as primary unstable product (VGO), primary plus secondary stable (gas, naphtha, kerosene, diesel).

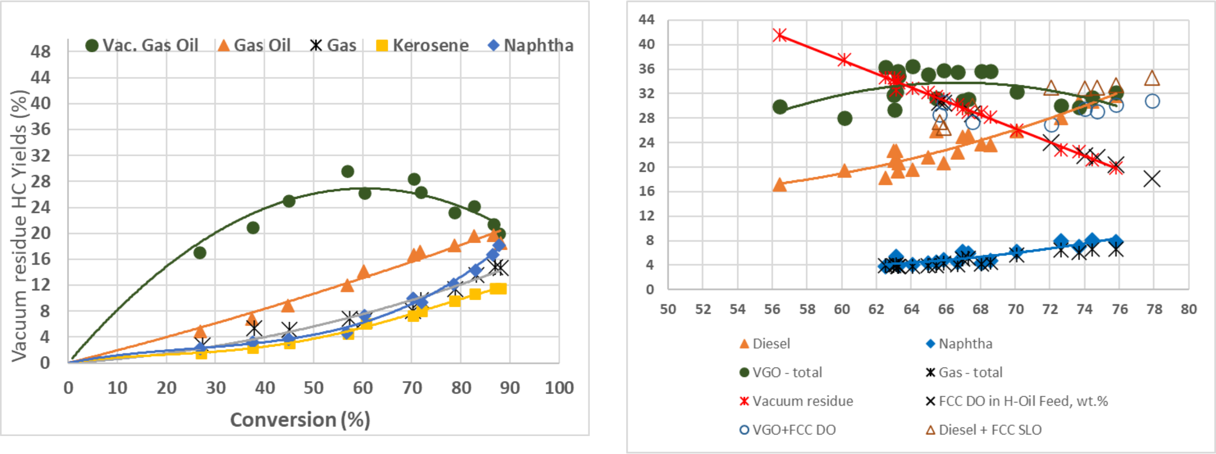

a

b

Figure 5. Selectivity curves of the vacuum residue hydrocracking obtained in a laboratory hydrocracking unit (a) (1-L semibatch magnetically stirred autoclave., as described in [48], and in the commercial LNB H-Oil VR hydrocracker (b) (313 t/h capacity)

Figure 5 b exhibits this product yields distribution, as obtained at the LNB H-Oil VR hydrocracker. The VGO yield, as mentioned above is a primary unstable product. With the increase of conversion initially the VGO yield increases, then it reaches its maximum, that is at a conversion level of about 66%, and beyond that conversion the VGO yield starts to decrease. The yields of gas, naphtha, and diesel, which are primary plus secondary stable products, always increase with augmentation of conversion. The unconverted vacuum residue (H-Oil vacuum tower bottom = VTB) always decreases with enhancement of conversion. There is a

Table 4. Properties of the three gas oils produced at LNB H-Oil VR hydrocracker obtained at different level of FCC SLO in the H-Oil VR feed

	H-Oil WABT 424 °C (4.05.2017) no SLO processed in H-Oil			H-Oil WABT 426 °C (09.05.2017) 8.3% SLO processed in H-Oil			H-Oil WABT 430 °C (01.08.2017) 9.5% SLO processed in H-Oil			H-Oil WABT 427 °C (14.08.2017) 6.1% SLO processed in H-Oil			H-Oil WABT 421 °C (08.09.2017) 4.1% SLO processed in H-Oil			H-Oil WABT 423 °C (15.09.2017) 5.9% SLO processed in H-Oil			H-Oil WABT 425 °C (21.01.2020) 11.9% SLO processed in H-Oil		
	no SLO	LVGO	HVGO	HAGO	LVGO	HVGO	HAGO	LVGO	HVGO	HAGO	LVGO	HVGO	HAGO	LVGO	HVGO	HAGO	LVGO	HVGO	HAGO	LVGO	HVGO
TRx H-Oil, oC	424	424	424	426	426	426	430	430	430	427	427	427	421	421	421	423	423	423	425	425	425
H-Oil Conversion %	72.5	72.5	72.5	75.3	75.3	75.3	74.3	74.3	74.3	72.7	72.7	72.7	67	67	67	68.9	68.9	68.9	77.2	77.2	77.2
FCC Conversion, %	73.20	73.20	73.20	71.5	71.5	71.5	70.11	70.11	70.11	72.6	72.6	72.6	74.2	74.2	74.2	70.7	70.7	7.07	73	73	73
FCC Slurry, t/h	0	0	0	20	20	20	25	25	25	12.5	12.5	12.5	10	10	10	15	15	15	22	22	22
FCC Slurry, %	0	0	0	8.25	8.25	8.25	9.45	9.45	9.45	6.1	6.1	6.1	4.13	4.13	4.13	5.87	5.87	5.87	11.9	11.9	11.9
Density at 15°C	0.9151	0.927	0.9437	0.9278	0.9428	0.954	0.9361	0.9573	0.9653	0.9295	0.9491	0.9573	0.9286	0.9422	0.9472	0.929	0.9449	0.9492	0.9442	0.9604	0.9652
HTSD ASTM D-7169, wt.%	°C	°C	°C	°C	°C	°C	°C	°C	°C	°C	°C	°C	°C	°C	°C	°C	°C	°C	°C	°C	°C
0.5	243	256	348	261	257	347	232	259	354	236	270	365	259	264	371	253	258	364	267	270	355
5	318	308	390	320	312	390	302	313	397	307	318	407	324	318	409	316	314	401	327	324	395
10	345	328	409	344	332	408	327	332	415	333	340	424	349	340	425	341	336	418	347	341	413
30	386	370	448	383	373	448	369	375	453	376	384	458	387	385	458	380	381	453	381	380	451
50	408	399	477	404	401	477	392	405	479	398	414	481	409	416	481	403	411	477	401	406	478
70	432	431	504	427	432	505	416	435	504	423	444	502	434	446	502	428	443	500	423	432	504
90	472	489	537	466	490	539	456	484	536	464	487	530	476	490	530	471	492	529	463	480	536
95	495	514	551	488	516	554	478	507	549	485	506	543	497	509	543	492	512	543	485	505	551
99.5	550	559	585	543	562	586	529	552	581	538	544	576	544	546	575	542	554	578	540	557	580
Boiling up to 360°C, wt.%	17.3	25.2	1.8	18.2	23.7	1.9	25.7	23.0	1.1	22.6	19.1	0.0	15.8	13.9	0.0	19.7	20.7	0.0	18.0	20.0	1.0

big scattering in the yields of VGO, and diesel, which can be explained with the different efficiency of the separation between the diesel and the VGO (HAGO, LVGO, and HVGO) product. Regardless of the data scattering for these yields (VGO and diesel) their selectivity curves coincides with those reported by Fukuyama and Terai [48]. Figure 5 b also includes data for the operation of the LNB H-Oil VR hydrocracker when FCC SLO is processed along with the VRO feed. The empty brown triangles designate the H-Oil diesel yield from the feed VR-FCC SLO feed, while the empty blue circles designate the H-Oil VGO yield from the same feed. The black crosses designate the H-Oil VTB yields obtained from the feed VR-FCC SLO feed. It is evident from this data set that in some cases the H-Oil diesel yield is higher than that of the feed 100% VRO, while in others the H-Oil diesel yield from the feed VR-FCC SLO feed fit to the selectivity curve of feed 100% VRO. The same is valid for the VGO yield. The VTB yield from the feed VR-FCC SLO feed lies completely of the curve of the feed 100% VRO which suggests different fractionation efficiency since the FCC slurry in its distillation characteristics pertains to the VGO cut and therefore its processing in the LNB H-Oil VR hydrocracker must lead to a lower VTB yield. As illustrated with the data in Figure 5b the fractionation efficiency of the LNB H-Oil VR hydrocracker has not been always the same. For that reason to discern the effect of any change in the feedstock or in the operating conditions on the product yields and selectivities dedicated test runs keeping the same efficiency of the fractionation should be performed.

3.3. Effect of the amount of FCC SLO in H-Oil feed on FCC conversion and FCC product yield structure

Having observed that the amount of FCC SLO in H-Oil feed has an effect on H-Oil VGO density it is easier to suggest that this will have also effect on the FCC conversion. The equation developed in our earlier work [50] to relate the H-Oil VGO conversion to the share of H-Oil VGO in FCCU feed and the FCCU conversion obtained during processing the blend of SRVGO and H-Oil VGO allows us to estimate the H-Oil VGO conversion.

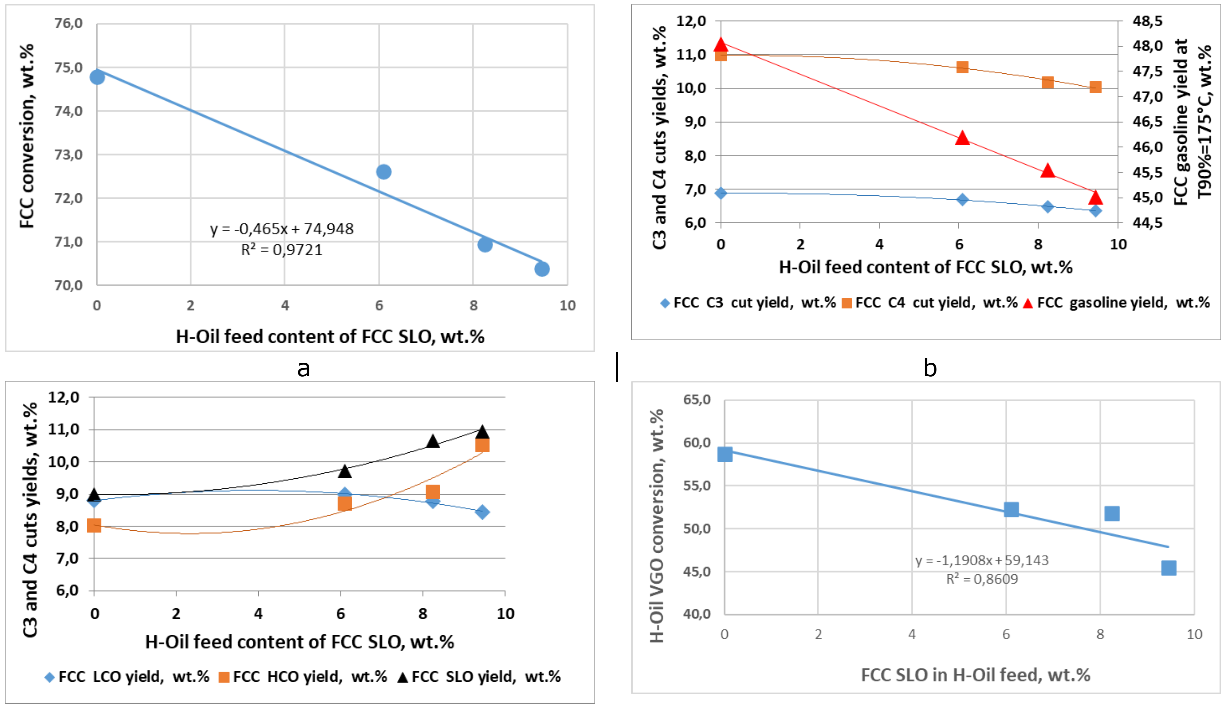

a

b

c

d

Figure 6. Dependence of FCCU conversion (a), and yields of C_3 cut, C_4 cut, gasoline (b), LCO, HCO, and SLO yields (c), and H-Oil VGO conversion on the content of FCC SLO in the H-Oil VR feed

Figure 6 summarizes the effect of H-Oil feed FCC SLO content on FCCU conversion (Figure 6 a), and yields of C_3 cut, C_4 cut, gasoline (Figure 6 b), LCO, HCO, and SLO yields (Figure 6c), and H-Oil VGO conversion. This data clearly indicates that the amount of FCC SLO processed in the H-Oil VR hydrocracker affects the performance of the FCCU. Therefore, a proper balance between the effect of FCC SLO on H-Oil hydrocracker performance and FCCU performance must be searched in order to optimize the whole refinery performance.

4. Conclusions

A literature survey on the properties of FCC SLO measured by NMR techniques, and liquid chromatography revealed that hydrogen content of the FCC SLO correlates with the aromatics content determined by SARA analysis, fraction aromatic carbon, determined by NMR, the average number of aromatic rings per molecule in FCC SLO, and the FCC SLO density. Analysis of FCC SLO samples taken at different FCC conversion levels did not show any effect of conversion on the FCC SLO properties in the FCC conversion range 72.47-82.4%.

The addition of about 8% FCC SLO to the H-Oil VR feed decreases sediments from 0.3 down to 0.1% even at increased WABT by 3°C. The distribution of FCC SLO among the H-Oil products was following: 15% in VTB; 60% in VGO, and 25% in diesel.

The increase of the amount FCC SLO in H-Oil feed decreases the FCC conversion, and the yields of the higher value products: C_3 cut, C_4 cut, and gasoline, and increases the yields of the lower value products: HCO, and SLO. An optimized balance between H-Oil VR hydrocracker and VGO FCCU performance related to the optimum amount of FCC SLO processed in the H-Oil could improve the performance of the whole refinery.

References

[1] Kalota S, Buckingham R. Make money in a slurry, Hydrocarbon Engineering, March (2013), http://www.ga.com/Websites/ga/images/products/gulftronic/pdf/Make_Money_in_a_Slurry.PDF

[2] Mondal S, Yadav A, Kumar R, Bansal V, Das SK, Christopher J, Kapur GS. Molecular-level structural insight into clarified oil by nuclear magnetic resonance (NMR) spectroscopy: Estimation of hydrocarbon types and average structural parameters. 2017; Energy Fuels 31(7): 7682-7692.

[3] Srivastava M, Kumar M, Singh R, Agarwal UC, Garg MO. Clarified oil from fluid catalytic cracking as an additional source of Group ii base oil components. Pet. Sci. Technol., 2011; 29 (2): 172.

[4] Guercio VJ. US producing, exporting more slurry oil. Oil and Gas Journal, 2010; 108(37): 96-99.

[5] Li W, Chen Y, Zhang L, Xu Z, Sun X, Zhao S, Xu C. Supercritical fluid extraction of FCC slurry oil: bulk property and molecular composition of narrow fraction. Energy Fuels, 2016; 30(12): 10064-10071.

[6] Stratiev D, Shishkova I, Tsaneva T, Mitkova M, Yordanov D. Investigation of relations between properties of vacuum residual oils from different origin, and of their deasphalted and asphaltene fractions. Fuel, 2016; 170: 115–129.

[7] Nesumi Y, Oyama T, Todo Y, Azuma A. Properties of fluid catalytic cracking decant oils of different origins in their single carbonization and cocarbonization with a petroleum vacuum residue. Ind. Eng. Chem. Res., 1990; 29: 1793-1801.

[8] Li W, Chen Y, Zhang L, Xu Z, Sun X, Zhao S, Xu C Supercritical fluid extraction of fluid catalytic cracking slurry oil: bulk property and molecular composition of narrow fractions. Energy Fuels,2016; 30(12): 10064-10071.

[9] Marques J, Maget S, Verstraete J. Improvement of ebullated-bed effluent stability at high conversion operation. Energy Fuels, 2011; 25: 3867–74.

[10] Marafi M, Al-Barood A, Stanislaus A. Effect of diluents in controlling sediment formation during catalytic hydrocracking of Kuwait vacuum residue. Pet. Sci. Technol., 2005; 23: 899-908.

[11] García FO, Juárez EM, Hernández PS. Controlling sediments in the ebullated bed hydrocracking process. Energy Fuels, 2012; 26: 2948−2952.

[12] Stratiev D, Dinkov R, Shishkova I, Sharafutdinov I, Ivanova N, Mitkova M, Yordanov D, Rudnev N, Stanulov K, Artemiev A, Barova I, and Chushkov B. What is behind the high values of hot filtration test of the ebullated bed residue H-Oil hydrocracker residual oils? Energy Fuels, 2016; 30: 7037–7054

[13] Stratiev D, Dinkov R, Shishkova I, Yordanov D. Can we manage the process of asphaltene precipitation during the production of IMO 2020 fuel oil?. submitted for publication.

[14] Wiehe IA Process Chemistry of Petroleum Macromolecules. Taylor & Francis Group, CRC Press, Boca Raton, 2008.

[15] Shuanglin Y, Jiling Z, Tao C, Lili R, Peng X, Honghong S. Effect of different aromatic fractions on colloidal property of TAHE atmospheric residue, China Petroleum Processing and Petrochemical Technology, 2012; 14(3): 17-23.

[16] Tirado A, Ancheyta J. A batch reactor study of the effect of aromatic diluents to reduce sediment formation during hydrotreating of heavy oil. Energy Fuels, 2018; 32(1): 60-66,.

[17] Lan X, Xu C, Wang G, Gao J. Reaction performance of FCC slurry catalytic cracking. Catal. Today 140 (2009) 174-178.

[18] Liu S, Xu Y. Exploration of the relationship between aromatics conversion and coking in catalytic cracking process. Acta Petrol. Sinica, 2013; 29: 145-150.

[19] Stratiev D, Shishkova I. Conversion of pyrolysis pitch and cycle oils in the fluid catalytic cracking, IPC2007 – 43rd International Petroleum Conference September 24–26, 2007, Bratislava, Slovak Republic.

[20] Shimada I, Takizawa K, Fukunaga H, Takahashi N, Takatsuka T. Catalytic cracking of polycyclic aromatic hydrocarbons with hydrogen transfer reaction, Fuel, 2015; 161: 207–214.

[21] Fang D, Wang G, Liu M, Nan J, Gao C, Gao J. Combined selective hydrogenation and catalytic cracking process for efficient conversion of heavy cycle oil to high octane number gasoline. Ind. Eng. Chem. Res., 2019; 58(43): 19752-19759,

[22] Fang D, Wang G, Sheng Q, Gea S, Gao C, Gao J. Preparation of hydrogen donor solvent for asphaltenes efficient liquid-phase conversion via heavy cycle oil selective hydrogenation. Fuel, 2019; 257: 115886.

[23] Xue Y, Yang J, Liu Z, Wang Z, Liu Z, Li Y, Zhang Y. Paving asphalt modifier from co-processing of FCC slurry with coal. Catalysis Today, 2014; 98: 333–338.

[24] Liang M, Liu S, Fan W, Xin X, Luo H, Xing B. Rheological and chemical characterization of deoiled asphalt modified with FCC slurry. Materials and Structures, 2015; 49(9):3607-3617.

[25] Cheng J, Xiang L, Liu K. The Characteristics of Asphalt Modified With FCC Slurry Oil. Pet. Sci. Technol., 2014; 32: 3010–3019.

[26] Wincek RT, Abrahamson JP, Eser S. Hydrodesulfurization of fluid catalytic cracking decant oils in a laboratory flow reactor and effect of hydrodesulfurization on subsequent coking. Energy Fuels, 2016; 30(8): 6281-6289.

[27] Abrahamson JP, Wincek RT, Eser S. Effects of catalyst properties on hydrodesulfurization activity for sulfur removal from fluid catalytic cracking decant oils. Energy Fuels, 2016; 30 (9): 7173-7179.

[28] Abrahamson JP, Wincek RT, Eser S. Scheme for hydrotreatment of fluid catalytic cracking decant oil with reduced hydrogen consumption and high needle coke yield upon carbonization. Energy Fuels, 2016; 30 (10): 8150-8155.

[29] B Fixari, P. Belloir, Le Perchec P. Coke production from an FCC-decant oil: characterization of the thermal process. Fuel, 1994; 73(8): 1284-1290.

[30] Park YD, Mochida I. A two-stage preparation of mesophase pitch from the vacuum residue of FCC decant oil. Carbon, 1989; 27(6): 925-929.

[31] US patent 9512319 Process for the production of carbon black from at least one FCC slurry cut, comprising a specific hydrotreatment_.

[32] Dong P, Wang C, Zhao S. Preparation of high performance electrorheological fluids with coke-like particles from FCC slurry conversion. Fuel, 2005; 84: 685–689.

[33] Lin Y, Nan G, Li Y, Luo H, Fan W. Ionic-liquid-catalyzed alkylation of extracted oil from a fluid catalytic cracking slurry. Energy Fuels, 2017; 31(11): 11911-11917.

[34] Song X, Liu D, Lou B, Li Zh, Guo A, Zhang D, Wang L. Removal of catalyst particles from fluid catalytic cracking slurry oil by the simultaneous addition of a flocculants and a weighting agent. Chem. Eng. Res. Des., 2018; 132: 686-696.

[35] Shishkova I, Stratiev D, Chavdarov I, Obryvalina A, Telyashev R, Mitkova M. 30 Years technology fluid catalytic cracking in LUKOIL Neftohim Burgas – Analysis of achieved progress Neftepererabotka i Neftohimia, 2015; 3, 3-18 (in Russian).

[36] Stratiev D, Shishkova I, Ivanov M, Chavdarov I, Yordanov D. FCC unit performance dependence on H-Oil severity, catalyst activity, and coke selectivity. submitted for publication.

[37] Stratiev D, Shishkova I, Yankov V, Kolev I, Mitkova M. Impact of H-Oil vacuum residue hydrocracking severity on fluid catalytic cracking unit performance. submitted for publication.

[38] Stratiev D, Shishkova I, Obryvalina A, Telyashev R. Feed properties impact on the Fluid Catalytic Cracking Unit - key issues in a diesel market. OGEM, 2011; 36(1): 25-28.
[39] Goossens AG. Prediction of molecular weight of petroleum fractions. Ind. Eng. Chem. Res., 1996; 35 (3): 985-988.
[40] Choudhary T, Meier P. Characterization of heavy petroleum feedstocks. Fuel Process. Technol., 2008; 89: 697-703.
[41] ASTM D5291 – 16, Standard test methods for instrumental determination of carbon, hydrogen, and nitrogen in petroleum products and lubricants.
[42] ASTM D2549 – 02 (2017), Standard test method for separation of representative aromatics and nonaromatics fractions of high-boiling oils by elution chromatography.
[43] Žajdlík R, Báhidský M. MCB utilisation for RHC unit operation and its impact on other unit performance, Criterion EB Workshop, San Diego 2015.
[44] Stratiev D, Shishkova I, Nikolaychuk E, Ilchev I, Yordanov D. Investigation of the effect of severity mode of operation in the H-Oil vacuum residue hydrocracking on sediment formation during processing different feeds. Pet Coal, 62(1): 50-62.
[45] Fukuyama H, Terai S. Kinetic Study on the Hydrocracking Reaction of Vacuum Residue Using a Lumping Model. Pet. Sci. Technol., 2007; 25(1-2): 277-287.
[46] Wallenstein D, Alkemade U. Modelling of selectivity data obtained from microactivity testing of FCC catalysts. Appl. Catal. A: Gen., 1996; 137: 37-54.

To whom correspondence should be addressed: professor Dr. Dicho Stratiev, LUKOIL Neftohim Burgas, Burgas 8104, Bulgaria, E-mail: Stratiev.dicho@neftochim.bg